Journal of Magnetic Resonance **147,** 121–128 (2000)
doi:10.1006/jmre.2000.2180, available online at http://www.idealibrary.com on IDEAL®

Analysis and Prediction of Isotropic Mixing Magnetization Transfer Profiles in Three-Spin Topologies

Sarata C. Sahu[1]

Department of Chemical Sciences, Tata Institute of Fundamental Research, Homi Bhabha Road, Mumbai 400 005, India

Received May 30, 2000; revised July 24, 2000

Isotropic mixing transfer functions (T_{kl}) in three-spin systems typical of amino acids have been analyzed in order to develop simple rules for predicting transfer maxima/minima. For certain topologies, the intrinsically complex expressions describing the transfer functions reduce to compact forms which are easy to interpret and analyze. For other topologies where compactification is not possible, an analysis of the component functions of the T_{kl} reveals that only one or two components contribute significantly to the overall profile of the transfer function. As a result, simple rules of the thumb may be devised for reasonably accurate prediction of mixing times corresponding to local and global transfer maxima/minima, thereby facilitating mixing time optimization in TOCSY experiments. © 2000 Academic Press

INTRODUCTION

The description of isotropic mixing (*1*) in multispin systems is essential for understanding and optimizing TOCSY (*1, 2*) experiments. Unlike pulsed-free-precession experiments, analytical descriptions of multispin coupling topologies are possible only for very special situations (*5–10*) and require numerical simulations in most cases (*11–17*). Excellent analysis of isotropic mixing has appeared in Refs. (*3*) and (*4*).

Recently, Glaser and co-workers have derived analytical expressions for isotropic mixing transfer functions T_{kl} in a general three-spin (AMX) system (*18*). It is obvious from the results that, except for very special cases, the T_{kl} are complicated sinusoidal functions of all relevant scalar couplings and the mixing time.

The rather complex nature of the transfer functions tends to reduce the utility of analytical expressions for predicting transfer maxima/minima, which is necessary for optimizing the mixing time in TOCSY experiments. Also, the complexity of the functions reveals very little insight into the dynamics of magnetization transfer in isotropic mixing. Any possibility of reducing these expressions to simpler forms or extracting their "key ingredients" to enhance their utility is always desirable.

In this paper, first we derive expressions for transfer functions in a general three-spin system using the relatively simple Liouville space framework, which is usually found in amino acid spin systems. Then, we consider topologies for which the expressions reduce to a compact form. As discussed below, these situations correspond to commonly observed scenarios in amino acids. For these topologies, transfer maxima and corresponding mixing times can be predicted precisely. We then go on to show that even for other three-spin topologies, which do *not* belong to such "compact" categories, considerable simplication is possible if we analyze the *component* functions of a given T_{kl}, rather than the function as a whole. As a result, mixing times corresponding to transfer maxima/minima (in other words, the mixing time *profile*) can still be predicted with a reasonable degree of accuracy, which is important from a practical standpoint.

ISOTROPIC MIXING IN A THREE-SPIN SYSTEM

For an arbitrary spin system $\{I_1, I_2, I_3\}$, the isotropic Hamiltonian is

$$H = 2\pi \sum_{k<l}^{3} J_{kl}\mathbf{I}_k \cdot \mathbf{I}_l. \quad [1]$$

Using the Liouville equation for the density operator σ, the time derivative for the expectation value of an operator A may be derived as

$$\dot{\sigma} = -i[H, \sigma] \quad [2]$$

$$\langle A\rangle = \mathrm{Tr}(A\sigma) \quad [3]$$

$$\langle \dot{A}\rangle = -\mathrm{i}\,\mathrm{Tr}\{A[H, \sigma]\}. \quad [4]$$

Using the property $\mathrm{Tr}\{A[B, C]\} = \mathrm{Tr}\{[A, B]C\}$, we have

$$\langle \dot{A}\rangle = -\mathrm{i}\,\mathrm{Tr}\{[A, H]\sigma\} \quad [5]$$

$$= -\mathrm{i}\langle [A, H]\rangle. \quad [6]$$

Using Eq. [6], the complete set of coupled differential equations maybe written down for an appropriate n-dimensional operator basis $\mathbf{A} \equiv \{A_k\}$, $k = 1, n$. An element A_k of this basis set is transformed by the commutator $[A_k, H]$ into a linear combination of the basis operators:

$$[A_k, H] = \sum_l R_{kl}A_l. \quad [7]$$

[1] Present address: Department of Biochemistry, University of California, Riverside, Riverside, CA 92521. E-mail: sarata@mail.ucr.edu.

1090-7807/00 $35.00

Therefore, we may write Eq. [6] in matrix form,

$$\frac{d\mathbf{A}}{dt} = -\mathrm{i}\mathbf{R}\mathbf{A}. \quad [8]$$

The isotropic Hamiltonian preserves coherence order. For a three-spin system, the following 15 normalized operators: I_x, S_x, Q_x, $2I_yS_z$, $2I_zS_y$, $2S_yQ_z$, $2S_zQ_y$, $2I_yQ_z$, $2I_zQ_y$, $4I_xS_yQ_y$, $4I_xS_zQ_z$, $4S_xI_yQ_y$, $4S_xI_zQ_z$, $4Q_xI_yS_y$, and $4Q_xI_zS_z$ represent an appropriate Liouville subspace. Differential equations can be written to describe the evolution of each of these operators. However, a suitable linear combination of these basis operators allows the set of 15 coupled differential equations to be partitioned into two sets of 9 and 6 equations each. The matrix equation for the nine-dimensional Liouville subspace is

$$\frac{d}{dt}\begin{pmatrix} \langle I_x\rangle - \langle S_x\rangle \\ \langle S_x\rangle - \langle Q_x\rangle \\ \langle I_x\rangle - \langle Q_x\rangle \\ IS \\ SQ \\ IQ \\ A-B \\ B-C \\ A-C \end{pmatrix} = \pi \begin{pmatrix} 0 & 0 & 0 & -2j_{12} & j_{23} & -j_{13} & 0 & 0 & 0 \\ 0 & 0 & 0 & j_{12} & -2j_{23} & -j_{13} & 0 & 0 & 0 \\ 0 & 0 & 0 & -j_{12} & -j_{23} & -2j_{13} & 0 & 0 & 0 \\ 2j_{12} & 0 & 0 & 0 & 0 & 0 & 0 & -j_{23} & j_{13} \\ 0 & 2j_{23} & 0 & 0 & 0 & 0 & -j_{12} & 0 & j_{13} \\ 0 & 0 & 2j_{13} & 0 & 0 & 0 & j_{12} & j_{23} & 0 \\ 0 & 0 & 0 & -j_{23}-j_{13} & 2j_{12}-j_{13} & j_{23}-2j_{12} & 0 & 0 & 0 \\ 0 & 0 & 0 & 2j_{23}-j_{13} & -j_{12}-j_{13} & j_{12}-2j_{23} & 0 & 0 & 0 \\ 0 & 0 & 0 & j_{23}-2j_{13} & j_{12}-2j_{13} & -j_{12}-j_{23} & 0 & 0 & 0 \end{pmatrix} \cdot \begin{pmatrix} \langle I_x\rangle - \langle S_x\rangle \\ \langle S_x\rangle - \langle Q_x\rangle \\ \langle I_x\rangle - \langle Q_x\rangle \\ IS \\ SQ \\ IQ \\ A-B \\ B-C \\ A-C \end{pmatrix}, \quad [9]$$

where j_{12}, j_{13} and j_{23} are the coupling constants between I, S; I, Q; S, Q, respectively, and

$$A = \langle I_xS_yQ_y\rangle + \langle I_xS_zQ_z\rangle \quad [10]$$

$$B = \langle S_xI_yQ_y\rangle + \langle S_xI_zQ_z\rangle \quad [11]$$

$$C = \langle Q_xI_yS_y\rangle + \langle Q_xI_zS_z\rangle \quad [12]$$

$$IS = \langle I_yS_z\rangle - \langle I_zS_y\rangle \quad [13]$$

$$SQ = \langle S_yQ_z\rangle - \langle S_zQ_y\rangle \quad [14]$$

$$IQ = \langle I_yQ_z\rangle - \langle I_zQ_y\rangle, \quad [15]$$

whereas the matrix equation for the six-dimensional subspace is

$$A^- = \langle I_xS_yQ_y\rangle - \langle I_xS_zQ_z\rangle \quad [17]$$

$$B^- = \langle S_xI_yQ_y\rangle - \langle S_xI_zQ_z\rangle \quad [18]$$

$$C^- = \langle Q_xI_yS_y\rangle - \langle Q_xI_zS_z\rangle \quad [19]$$

$$IS^+ = \langle I_yS_z\rangle + \langle I_zS_y\rangle \quad [20]$$

$$SQ^+ = \langle S_yQ_z\rangle + \langle S_zQ_y\rangle \quad [21]$$

$$IQ^+ = \langle I_yQ_z\rangle + \langle I_zQ_y\rangle. \quad [22]$$

Interestingly, both sets of equations are amenable to analytical solutions using standard methods, such as Laplace transforms or matrix diagonalization. We found the Laplace transform method more easy to implement on *Mathematica* version 2.2. While the procedure is standard textbook material, it is outlined below for completeness. Taking Laplace transforms on both sides of Eq. [6] we have

$$s\mathscr{L}_A - \mathbf{A}(0) = -\mathrm{i}\mathbf{R}\mathscr{L}_A, \quad [23]$$

$\mathscr{L}_A$ being the Laplace transform of **A**. After rearranging Eq. [23], we have

$$(s\mathbf{E} + i\mathbf{R})\mathscr{L}_A = \mathbf{A}(0), \quad [24]$$

where **E** is the identity operator. Denoting $\mathbf{U} = s\mathbf{E} + \mathrm{i}\mathbf{R}$, we have

$$\frac{d}{dt}\begin{pmatrix} IS^+ \\ SQ^+ \\ IQ^+ \\ A^- \\ B^- \\ C^- \end{pmatrix} = \pi \begin{pmatrix} 0 & 0 & 0 & -j_{13} & -j_{23} & j_{23}+j_{13} \\ 0 & 0 & 0 & -j_{12} & j_{12}+j_{23} & -j_{23} \\ 0 & 0 & 0 & j_{12}+j_{13} & -j_{12} & -j_{13} \\ j_{13} & j_{12} & -j_{12}-j_{13} & 0 & 0 & 0 \\ j_{23} & -j_{12}-j_{23} & j_{12} & 0 & 0 & 0 \\ -j_{23}-j_{13} & j_{23} & j_{13} & 0 & 0 & 0 \end{pmatrix} \cdot \begin{pmatrix} IS^+ \\ SQ^+ \\ IQ^+ \\ A^- \\ B^- \\ C^- \end{pmatrix}, \quad [16]$$

TABLE 1
Expressions of Transfer Functions for Isotropic Mixing in a General Three-Spin System

$$\langle T\rangle_{11} = \frac{1}{3} + \frac{(j_{12}+2j_{23}+j_{13})^2}{18D^2} + \frac{(j_{13}-j_{12})^2}{6D^2}\cos\lambda_1 t + \frac{2D-j_{12}+2j_{23}-j_{13}}{9D}\cos\lambda_2 t + \frac{2D+j_{12}-2j_{23}+j_{13}}{9D}\cos\lambda_3 t$$

$$\langle T\rangle_{12} = \frac{1}{3} + \frac{(j_{12}+j_{23}-2j_{13})\cdot(j_{12}-2j_{23}+j_{13})}{18D^2} + \frac{(j_{12}-j_{23})\cdot(j_{13}-j_{12})}{6D^2}\cos\lambda_1 t + \frac{2j_{12}-j_{23}-j_{13}-D}{9D}\cos\lambda_2 t + \frac{-2j_{12}+j_{23}+j_{13}-D}{9D}\cos\lambda_3 t$$

$$\langle T\rangle_{13} = \frac{1}{3} + \frac{(j_{12}+2j_{23}+j_{13})\cdot(-2j_{12}+j_{23}+j_{13})}{18D^2} + \frac{(j_{23}-j_{13})\cdot(j_{13}-j_{12})}{6D^2}\cos\lambda_1 t + \frac{-j_{12}-j_{23}+2j_{13}-D}{9D}\cos\lambda_2 t + \frac{j_{12}+j_{23}-2j_{13}-D}{9D}\cos\lambda_3 t$$

Note. $d = (j_{12}+j_{23}+j_{13})$; $D = (j_{12}^2+j_{23}^2+j_{13}^2-(j_{12}j_{23}+j_{23}j_{13}+j_{12}j_{13}))^{1/2}$; $\lambda_1 = 2\pi D$; $\lambda_2 = \pi(d-D)$; $\lambda_3 = \pi(d+D)$.

$$\mathcal{L}_A = \mathbf{U}^{-1}\mathbf{A}(0) \quad [25]$$

and, consequently,

$$\mathbf{A}(t) = \mathbf{V}\mathbf{A}(0) \quad [26]$$

$$\mathbf{V} = \mathcal{L}^{-1}\mathbf{U}^{-1}. \quad [27]$$

Here we present results obtained for the usually encountered initial condition where the magnetization resides in-phase on one of the spins. This results in only the nine-dimensional subspace being relevant for the solutions. The expressions for transfer functions pertaining to in-phase and two-spin antiphase operators are listed in Tables 1 and 2, respectively. Using accepted conventions, we use the symbol T_{kl} to denote the $k \rightarrow l$ transfer function which, in the Liouville space formalism, corresponds to the value of $\langle A_l\rangle(t)$ for the initial condition $\langle A_k\rangle(0) = 1$, others zero. From the expression for T_{kl}, other transfer functions (e.g., T_{lm}) may be obtained by simple permutation of the spin identities.

The three-spin topology found typically in biomolecules consists of two vicinal and one geminal coupling (Fig. 1), usually an H_α–$H_{\beta 1}$–$H_{\beta 2}$ system in Phe, Tyr, Trp, His, Asp, Asn, Cys, and Ser. In this work, we refer to the vicinal $J_{\alpha\beta 1,2}$ as v_1 (j_{12}) and v_2 (j_{13}), respectively, and the geminal $J_{\beta 1\beta 2}$ coupling as g (j_{23}), with $\{v_1, v_2\} \leq |g|$. The validity of the conclusions made in this paper has been tested for $0 \leq \{v_1, v_2\} \leq 15$ Hz and $-16 < g < -12$, which are the usually observed ranges of these couplings in amino acids (*20–23*). For the simulations shown in the paper, we have assumed a value of -15 Hz for g. Finally, we have concentrated only on "cross-peak intensities," i.e., T_{kl}, $k \neq l$.

ANALYSIS OF TOPOLOGIES YIELDING COMPACT SOLUTIONS

In general, the total transfer function $T_{kl}(\tau_m)$ for an n-spin system is given by (*4*)

$$T_{kl}(\tau_m) = a_0 + \sum_{j=1}^{N} f_j(\tau_m) \quad [28]$$

$$f_j(\tau_m) = a_j \cdot \cos(2\pi\nu_j\tau_m), \quad [29]$$

where $N = 1$ and 3 for two- and three-spin systems, respectively, and ν_j are derived from differences of eigenvalues of H. The number N grows rapidly with the number of spins in the network (e.g., $N = 12$ for a four-spin system) (*19*).

Since T_{kl} is a superposition of several trigonometric functions, it is not trivial to calculate maxima and minima even if all the a_j and ν_j are known. However, for certain spin topologies, the individual functions f_j seldom contribute equally to T_{kl}, which then becomes far more tractable for analysis.

From Eq. [29], the vicinal transfer function T_{12} for a three-spin system may be written as

$$T_{12}(\tau_m) = a_0 + f_1(\tau_m) + f_2(\tau_m) + f_3(\tau_m). \quad [30]$$

Based on the results of Table 1 and with $v_{1,2}$ as defined above, the coefficients a_j and functions f_j are

$$a_0 = 1/3 + (v_1+v_2-2g)(v_1-2v_2+g)/(18D^2) \quad [31]$$

$$f_1 = a_1 \cdot \cos(2\pi D\tau_m) \quad [32]$$

$$f_2 = a_2 \cdot \cos[\pi(d-D)\tau_m] \quad [33]$$

$$f_3 = a_3 \cdot \cos[\pi(d+D)\tau_m] \quad [34]$$

$$a_1 = \frac{(v_1-v_2)(g-v_1)}{6D^2} \quad [35]$$

$$a_2 = \frac{(2v_1-v_2-g-D)}{9D} \quad [36]$$

$$a_3 = \frac{-(2v_1-v_2-g+D)}{9D} \quad [37]$$

$$d = g + v_1 + v_2 \quad [38]$$

$$D = [g^2+v_1^2+v_2^2-(gv_1+gv_2+v_1v_2)]^{1/2}. \quad [39]$$

T_{13} and T_{23} are obtained easily from Eqs. [31]–[39], by appropriately permuting the identities of the spins. Two situations where T_{12} takes a simple form are the following.

TABLE 2
Expressions for Transfer Coefficients for Transfer from $I_x \rightarrow$ Different Antiphase Terms for Isotropic Mixing in a General Three-Spin System

$$\langle 2I_yS_z\rangle = -\langle 2I_zS_y\rangle = \frac{((j_{12}-j_{13})\sin\lambda_1 + (-j_{12}+j_{23}+D)\sin\lambda_2 + (j_{12}-j_{23}+D)\sin\lambda_3)}{6D}$$

$$\langle 2S_yQ_z\rangle = -\langle 2S_zQ_y\rangle = \frac{(j_{12}-j_{13})\cdot(\sin\lambda_1 + \sin\lambda_2 - \sin\lambda_3)}{6D}$$

$$\langle 2I_yQ_z\rangle = -\langle 2I_zQ_y\rangle = \frac{((j_{13}-j_{12})\sin\lambda_1 + (j_{23}-j_{13}+D)\sin\lambda_2 + (-j_{23}+j_{13}+D)\sin\lambda_3)}{6D}$$

$$\langle I_xS_zQ_z\rangle = \langle I_xS_yQ_y\rangle = -\frac{(j_{12}-2j_{23}+j_{13})^2}{18D^2} - \frac{(j_{13}-j_{12})^2}{6D^2}\cos\lambda_1 + \frac{(2D-j_{12}+2j_{23}-j_{13})}{18D}\cos\lambda_2 + \frac{(2D+j_{12}-2j_{23}+j_{13})}{18D}\cos\lambda_3$$

$$\langle S_xI_zQ_z\rangle = \langle S_xI_yQ_y\rangle$$
$$= \frac{(j_{12}-2j_{23}+j_{13})\cdot(-j_{12}-j_{23}+2j_{13})}{18D^2} + \frac{(j_{23}-j_{12})\cdot(j_{13}-j_{12})}{6D^2}\cos\lambda_1 + \frac{(2j_{12}-j_{23}-j_{13}-D)}{18D}\cos\lambda_2 + \frac{(-2j_{12}+j_{23}+j_{13}-D)}{18D}\cos\lambda_3$$

$$\langle Q_xI_zS_z\rangle = \langle Q_xI_yS_y\rangle$$
$$= \frac{(2j_{12}-j_{23}-j_{13})\cdot(j_{12}-2j_{23}+j_{13})}{18D^2} + \frac{(j_{12}-j_{13})\cdot(j_{23}-j_{13})}{6D^2}\cos\lambda_1 + \frac{(-j_{12}-j_{23}+2j_{13}-D)}{18D}\cos\lambda_2 + \frac{(j_{12}+j_{23}-2j_{13}-D)}{18D}\cos\lambda_3$$

Note. d, D, λ_1, λ_2, and λ_3 are as defined for Table 1.

(a) $\nu_1 = \nu_2 = \nu$

This has been dealt with in detail by Glaser (*9*) and corresponds to gauche–gauche or rotationally averaged conformations in amino acid side chains. $T_{12} = T_{13}$ takes the form

$$T_{12} = T_{13} = \frac{2}{9}[1 - 2\cos(3\pi\nu t)]. \qquad [40]$$

As noted by Glaser (*9*), the transfer is independent of g. Transfer maxima ($T_{12}^{\max} = T_{13}^{\max} = 33\%$) appear at odd multiples of $t = 1/(3\nu)$.

(b) $d \sim 0$, ***or*** $d/D \ll 1$, ***i.e.,*** $g \approx -(\nu_1 + \nu_2)$

This is not an uncommon situation in amino acids, typical examples being the *trans*-gauche conformation ($\nu_1 = 3$, $\nu_2 = 12$, $g = -15$) or ($\nu_1 = 6$, $\nu_2 = 9$, $g = -15$) (*20*). Considering the situation where d is exactly zero, the expressions for T_{12} and T_{13} become

$$T_{12} = \frac{1}{3} - \frac{\nu_2(\nu_1+\nu_2)}{2D^2} + \frac{(2\nu_1+\nu_2)(\nu_2-\nu_1)}{6D^2} \times \cos 2\pi Dt - \frac{2}{9}\cos\pi Dt \qquad [41]$$

$$T_{13} = \frac{1}{3} - \frac{\nu_1(\nu_2+\nu_1)}{2D^2} - \frac{(2\nu_2+\nu_1)(\nu_1-\nu_2)}{6D^2} \times \cos 2\pi Dt - \frac{2}{9}\cos\pi Dt \qquad [42]$$

$$D = [3(\nu_1^2 + \nu_2^2 + \nu_1\nu_2)]^{1/2}. \qquad [43]$$

By setting the time derivatives to zero, it is easily shown that for $z = (\nu_1/\nu_2) < (1 + \sqrt{3})$, extrema correspond to

$$\sin\pi D\tau_m^{\max} = 0 \quad z = \nu_1/\nu_2 < (1 + \sqrt{3}). \qquad [44]$$

The interesting point to note here is that for both T_{12} and T_{13}, peak (maxima or in some cases local minima) appear at the same mixing time ($1/D$), with identical efficiencies of 44.4%, regardless of the relative magnitudes of ν_1 and ν_2. As a result, both of the cross peaks can be maximized at the same mixing time. T_{23} also has the same value (44.4%) at $t = 1/D$, although it does not correspond to a maximum. This is illustrated in Fig. 2a, which shows the three transfer functions, assuming $\nu_1 = 9.0$ and $\nu_2 = 6.0$ Hz. T_{12}, associated with the larger coupling ν_1, builds up

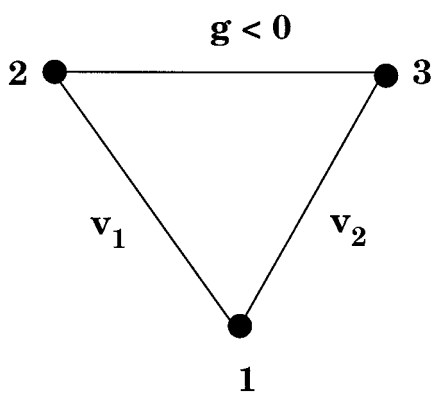

FIG. 1. A general three-spin system typically seen in biomolecules. Here ν_1 and ν_2 are vicinal and g is the geminal coupling constant.

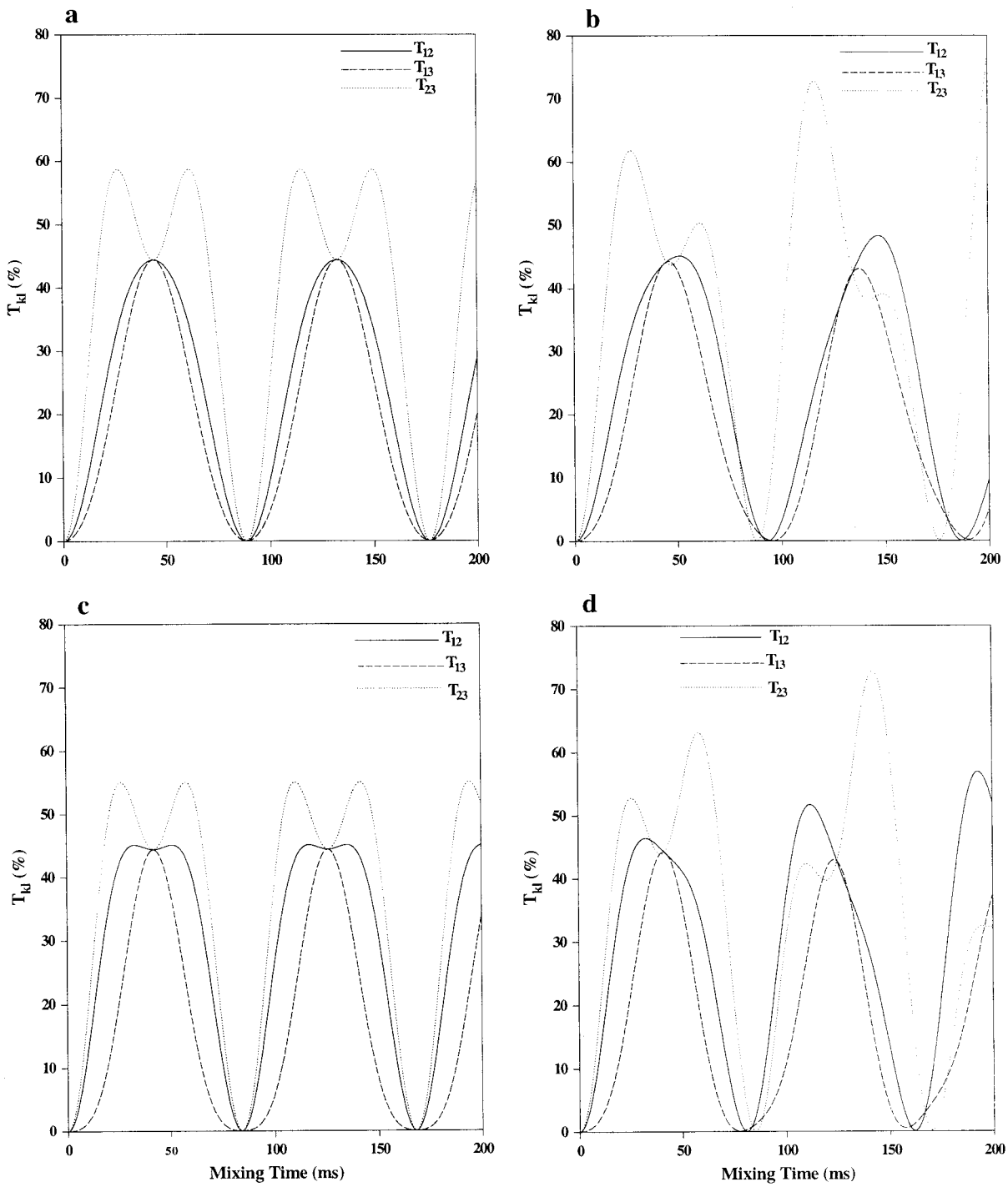

FIG. 2. Mixing time dependence of transfer functions at different values of ν_1 and ν_2: (a) $\nu_1 = 9.0$ Hz and $\nu_2 = 6.0$ Hz, (b) $\nu_1 = 9.0$ Hz and $\nu_2 = 4.0$ Hz, (c) $\nu_1 = 12.0$ Hz and $\nu_2 = 3.0$ Hz, (d) $\nu_1 = 12.0$ Hz and $\nu_2 = 3.5$ Hz. The value of g is -15 Hz in all cases.

rapidly in the beginning, but the slower function T_{13} catches up steeply in the vicinity of $t = 1/D$. In situations where $d \neq 0$ but $d \ll D$, the maxima of T_{12} and T_{13} are marginally offset from each other, but the point of intersection lies very close to the larger/smaller of the two peaks, as shown in Fig. 2b ($\nu_1 = 9.0$, $\nu_2 = 4.0$, $d/D = -0.09$). In addition, T_{23} develops multiple maxima, which exceed that of T_{12} and T_{13}.

For $z \geq (1 + \sqrt{3})$, the condition for extrema is given by

$$\cos \pi D \tau_m^{\max} = \frac{\nu_1^2 + \nu_2^2 + \nu_1\nu_2}{(\nu_2 - \nu_1)(2\nu_1 + \nu_2)} \quad z \geq (1 + \sqrt{3}). \quad [45]$$

An example of the mixing time profile of a topology in this

category ($v_1 = 12$, $v_2 = 3$) is shown in Fig. 2c. T_{12} displays multiple maxima at

$$\tau_m^{max} = \frac{1}{\pi D}\left[2n\pi \pm \arccos\left\{\frac{v_1^2 + v_2^2 + v_1 v_2}{(v_2 - v_1)(2v_1 + v_2)}\right\}\right]$$
$$n = 1, 2, \ldots \quad [46]$$

Since the condition in Eq. [45] requires one vicinal coupling to be almost four times the other, it occurs only for classic *trans*-gauche conformations. The T_{12} and T_{13} curves meet at $1/D$, which is a T_{12} local minimum sandwiched between the two symmetrical T_{12} maxima. If d deviates slightly from zero as shown in Fig. 2d ($v_1 = 12$, $v_2 = 3.5$, $d/D = 0.02$), the T_{12} profile becomes skewed, but the overall profile remains similar.

ANALYSIS OF TOPOLOGIES WITHOUT COMPACT SOLUTIONS

For topologies which do not belong to either of the above two categories, it is still possible to predict the profile of T_{kl} vs τ_m with reasonable accuracy, over the vicinal coupling constant range $0 \leq \{v_1, v_2\} \leq 15$ Hz. Figures 3a–3d show T_{12} and T_{13} for two topologies for which $v_1 \neq v_2$ and neither is $v_1 + v_2 \sim |g|$. In each of the plots, the T_{kl}, f_1, f_3, and $Q_{kl} = f_1 + f_3$ are shown as a function of mixing time. It is easily seen that the sum (Q_{kl}) of the fastest frequency component (f_1) and the largest amplitude component (f_3) reproduce the overall profile of T_{kl} very closely. While it is easily demonstrated from the definitions of d and D that f_1 is the most rapidly oscillating component for all v_1, v_2, and g, a_3 is not always the largest coefficient. However, numerical calculations show that a_3 is indeed the largest coefficient in the range $0 \leq \{v_1, v_2\} \leq 15$. Although a value of $g = -15$ Hz has been used in Fig. 3, the validity of the result has been verified over the range $12 < |g| < 16$.

Essentially, a knowledge of the extrema of f_1 (at multiples of $1/D$) and f_3 (at multiples of $2/(d + D)$) is a good indicator of the profile of the overall function. Two different situations may be considered, as follows.

$v_1 + v_2 < |g|$. Each local maximum or minimum of T_{kl} usually coincides with corresponding extrema of f_1. If $v_1 < v_2$ (Fig. 3a), a_1 is positive (Eq. [35]) and, therefore, f_1 maxima occur at $t_{f1}^{max} = n/D$, $n = 1, 2, \ldots$. If $v_1 > v_2$, a_1 is negative and, therefore, f_1 maxima appear at $t_{f1}^{max} = (2n - 1)/(2D)$, $n = 1, 2, \ldots$. For $v_1 < v_2/2$, a_3 is obviously negative (Eq. [37]). Otherwise, a_3 becomes positive only when $(v_2 - 2v_1) > (|g| + D)$. Both $|g|$ and D are large quantities and, therefore, this condition requires v_2 to be abnormally large, which is never true for any realistic values of proton coupling constants. As a result, a_3 may be considered negative and, therefore, f_3 maxima appear at $t_{f3}^{max} = (2n - 1)/(d + D)$.

"Global" maxima in T_{kl} arise when f_1 and f_3 are maximally in-phase, i.e., when maxima of f_1 coincide with that of f_3. When f_1 and f_3 are anti-phase, i.e., an f_1 maximum coincides with an f_3 minimum, the situation corresponds to a global *minimum* in T_{kl}, since a_3 is always the more dominant coefficient. From a practical viewpoint, these observations may be encapsulated into the following protocol: Tabulate all values of t_{f1}^{max}, t_{f1}^{min}, t_{f3}^{max}, and t_{f3}^{min} in a given mixing time range. In general, a t_{f1}^{max} corresponds to a local maximum in the T_{kl}. If the t_{f1}^{max} also happens to be coincident with or appears close to a t_{f3}^{max}, the situation corresponds to a global maximum. On the other hand, if $t_{f1}^{max}/t_{f1}^{min}$ lies close to a t_{f3}^{min}, a global minimum results.

When $v_1 + v_2 > |g|$ (Figs. 3c and 3d), the denominator of a_1 ($6D^2$) becomes large and, therefore, a_1 is small. The T_{kl} profile is, therefore, almost completely dominated by f_3. Maxima and minima in T_{kl} appear at mixing times close to $t_{f3}^{max} = (2n - 1)/(d + D)$. The f_3 maxima are broad, typically spanning 10 ms. As a result, differences between the value of T_{kl} at t_{f3}^{max} and the actual T_{kl}^{max} is very small (Figs. 3c and 3d) and largely insensitive to the relative magnitudes of v_1 and v_2.

Combining the compact solutions with the "rules" developed in this section, mixing times corresponding to transfer function maxima/minima may be obtained largely from a knowledge of d and D alone.

CONCLUSIONS

The isotropic mixing transfer functions in three-spin systems are obtained using an alternative approach to that of Glaser *et al.* (*18*) and analyzed these functions in order to extract their information content in a simple manner. For certain spin topologies typical of amino acids, the intrinsically complex functions reduce to compact forms which are easy to use for predicting transfer maxima/minima. An interesting result occurs when $v_1 + v_2 \sim |g|$, wherein both the transfer functions T_{12} and T_{13} peak at the same mixing time with the same value, regardless of the relative magnitudes of v_1 and v_2. For other topologies where compactification is not possible, in the normally observed coupling constant ranges of $0 \leq \{v_1, v_2\} \leq 15$ Hz and $-16 \leq g \leq -12$, an analysis of the component functions of the T_{kl} reveals that only one or two components contribute significantly to the overall profile of the transfer function. This leads to simple rules of the thumb for reasonably accurate prediction of mixing times corresponding to local and global transfer maxima/minima and thereby facilitates mixing time optimization in experiments. The transfer functions presented in this paper corespond to the ideal isotropic mixing case, where effect relaxation is neglected, which often leads to an additional damping of the experimental transfer function. In practice, relaxation effects are more severe at longer mixing times and need to be accounted for. However, for small to medium-size molecules in which proton TOCSY experiments are most relevant, these expressions are likely to be applicable up to 100 ms of mixing time, depending on

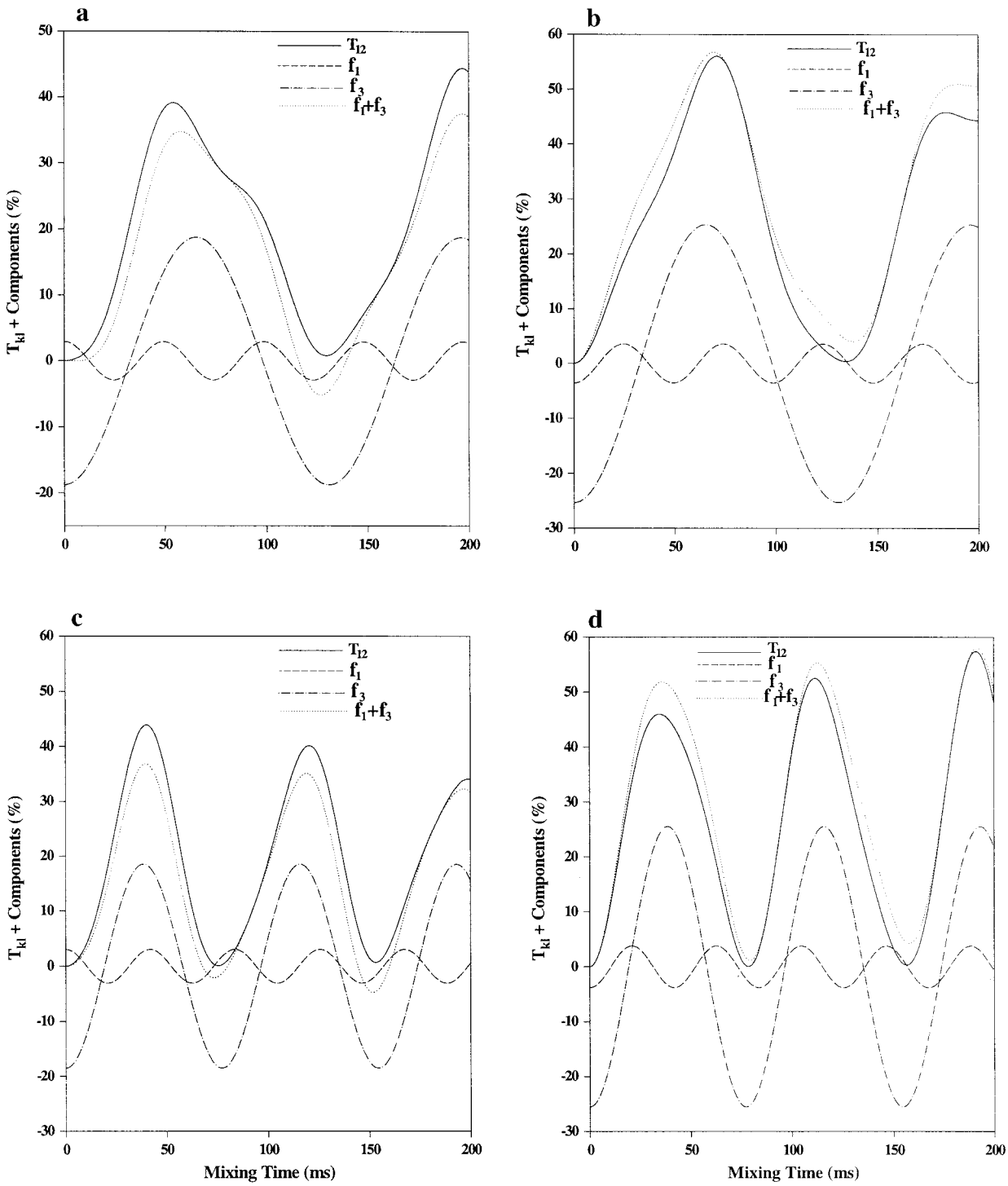

FIG. 3. Mixing time dependence of transfer functions and their various components at different values of ν_1 and ν_2: (a) ν_1 = 3.0 Hz and ν_2 = 7.0 Hz, (b) ν_1 = 7.0 Hz and ν_2 = 3.0 Hz, (c) ν_1 = 6.0 Hz and ν_2 = 11.0 Hz, (d) ν_1 = 11.0 Hz and ν_2 = 6.0 Hz. The value of g is always taken as −15 Hz.

the molecular weight. While this analysis has been restricted to the smallest of multispin systems, investigation of isotropic mixing in four-spin systems has indicated that even when the number of component functions increases significantly (12 for 4-spin systems), about 6 of 12 harmonic terms contribute substantially to the overall T_{kl} (*19*). This holds out promise for similar analyses of more complex spin systems.

ACKNOWLEDGMENT

I thank Dr. Ananya Majumdar for his constant support, suggestions, and many useful discussions.

REFERENCES

1. L. Braunschweiler and R. R. Ernst, Coherence transfer by isotropic mixing: Application of proton correlation spectroscopy, *J. Magn. Reson.* **53,** 521–528 (1983).
2. A. Bax and D. G. Davis, MLEV-17-based two-dimensional homonuclear magnetization transfer spectroscopy, *J. Magn. Reson.* **65,** 355–360 (1985).
3. S. J. Glaser and G. P. Drobny, *in* "Advances in Magnetic Resonance," (J. S. Waugh, Ed.), Vol. 14, p. 35–58, Academic Press, San Deigo.
4. S. J. Glaser and J. J. Quant, *in* "Advances in Magnetic and Optical Resonance," (W. S. Warren, Ed.), Vol. 19, pp. 59–252, Academic Press, San Diego.
5. N. Chandrakumar and S. Subramanian, Some aspects of coherence transfer by isotropic mixing, *J. Magn. Reson.* **62,** 346–349 (1985).
6. N. Chandrakumar, G. V. Visalakshi, D. Ramaswamy, and S. Subramanian, Analysis of collective modes in some A_MX_N systems, *J. Magn. Reson.* **67,** 307–318 (1986).
7. G. V. Visalakshi and N. Chandrakumar, Automated generation of commutators algebra for NMR problems, *J. Magn. Reson.* **75,** 1–8 (1987).
8. J. Listerud, S. J. Glaser, and G. P. Drobny, Symmetry and isotropic coherence transfer; II. Multi spin calculations using a young tableaux formulation, *Mol. Phys.* **78,** 629–658 (1993).
9. S. J. Glaser, Coupling topology dependence of polarization-transfer efficiency in TOCSY and TACSY experiments, *J. Magn. Reson. A* **104,** 283–301 (1993)
10. A. Majumdar, Analytical expressions for isotropic mixing in three- and four-spin topologies in ^{13}C systems, *J. Magn. Reson. A* **121,** 121–126 (1996).
11. M. Rance, Sign reversal of resonances via isotropic mixing in NMR spectroscopy, *Chem. Phys. Lett.* **154,** 242–247 (1989).
12. M. L. Remerowski, S. J. Glaser, and G. P. Drobny, A theoretical study of coherence transfer by isotropic mixing; Calculation of pulse sequence performance for systems of biological interest, *Mol. Phys.* **68,** 1191–1218 (1989).
13. J. Cavanagh, W. J. Chazin, and M. Rance, The time dependence of coherence transfer in homonuclear isotropic mixing experiments, *J. Magn. Reson.* **87,** 110–131 (1990).
14. A. Bax, G. M. Clore, and A. M. Gronenborn, ^{1}H–^{1}H correlation via isotropic mixing of ^{13}C magnetization—A new three-dimensional approach for assigning ^{1}H and ^{13}C spectra of ^{13}C-enriched proteins, *J. Magn. Reson.* **88,** 425–431 (1990).
15. H. S. Eaton, S. W. Fesik, S. J. Glaser, and G. P. Drobny, Time dependence of ^{13}C–^{13}C magnetization transfer in isotropic mixing experiments involving amino acid spin systems, *J. Magn. Reson.* **90,** 452–463 (1990).
16. S. S. Wijmenga, H. A. Heus, B. Werten, G. A. van der Marel, J. H. van Boom, and C. W. Hilbers, Assignment strategies and analysis of cross-peak patterns and intensities in the three-dimensional homonuclear TOCSY-NOESY of RNA, *J. Magn. Reson. B* **103,** 134 (1994).
17. P. Khandelwal, A. Majumdar, and R. V. Hosur, Mixing time dependence of cross peak intensities in ^{13}C resolved ^{1}H–^{1}H TOCSY spectra of proteins, *Proc. Natl. Acad. Sci. India* **66**(A), Special Issue, 1996.
18. O. Schedletzsky and S. J. Glaser, Analytical coherence-transfer functions for the general AMX spin system under isotropic mixing, *J. Magn. Reson. A* **123,** 174–180 (1996).
19. B. Luy, O. Schedletzsky, and S. J. Glaser, Analytical polarization transfer functions for four coupled spins $\frac{1}{2}$ under isotropic mixing conditions, *J. Magn. Reson. A* **138,** 19–27 (1999).
20. H. Widmer and K. Wuthrich, Simulated two-dimensional NMR cross-peak fine structures for ^1H spin systems in polypeptides and polydeoxynucleotides, *J. Magn. Reson.* **74,** 316–336 (1987).
21. K. Bartik and C. Redfield, A method for the estimation of ^{x}1 torsion angles in proteins, *J. Biomol. NMR* **3,** 415–428 (1993).
22. M. Cai, J. Liu, Y. Gong, and R. Krishnamoorthi, A practical method for stereospecific assignments of γ- and δ-methylene hydrogens via estimation of vicinal ^{1}H–^{1}H coupling constants, *J. Magn. Reson. B* **107,** 172–178 (1995).
23. K. L. Constantine, M. S. Friedrichs, and L. Mueller, Simple approaches for estimating vicinal ^{1}H–^{1}H coupling constants and for obtaining stereospecific resonance assignments in leucine side chains, *J. Magn. Reson. B* **104,** 62–68 (1994).
24. J. Briandt and R. R. Ernst, Sensitivity comparison of two-dimensional correlation spectroscopy in the laboratory frame and in the rotating frame, *J. Magn. Reson. A* **104,** 54–62 (1993).